Accepted manuscript doi:
10.1680/jgeen.17.00131

Submitted: 09 July 2017

Published online in 'accepted manuscript' format: 09 March 2018

Manuscript title: Behaviour of normally consolidated clay containing isolated solid inclusions

Authors: Vinayagamoorthy Sivakumar[1], Shane Donohue[2], Laura Henderson[3], Satyajeet Nanda[4] and Snehasis Tripathy[5]

Affiliations: [1]Queen's University Belfast, UK; [2]University College Dublin, Ireland; [3]NTNU, Norway; [4]KIIT Bhubaneswar, India; [5]Cardiff University, UK

Corresponding author: Vinayagamoorthy Sivakumar, School of Natural and Built Environment, Queen's University Belfast, BT7 1NN, UK. Tel.: 028 90974009.

E-mail: v.sivakumar@qub.ac.uk

Accepted manuscript doi:
10.1680/jgeen.17.00131

Abstract

This paper examines the compression and strength characteristics of soils in relation to the presence of isolated solid inclusions such as colluvium and glacial till. Investigations were carried out on samples of kaolin with solid inclusions of angular crushed basalt and steel ball bearings (to represent rounded particles). It was observed that the presence of solid inclusions has a significant effect on the compression and strength characteristics of these composite soils and it is postulated that this behaviour is related to the formation of strong arches between the individual solid inclusions. This phenomenon was found to be subdued when the surface of the solid inclusion is smooth, suggesting that particle shape has also considerable influence on the mechanical behaviour of composite materials.

Keywords: Clay, strength, compressibility

Accepted manuscript doi:
10.1680/jgeen.17.00131

INTRODUCTION

The engineering behaviour of natural soils is dependent on the constituent particles shape, size, arrangement, bonding and mineralogy as well as interactions at the particulate level (Olson and Mesri, 1970; Clemence and Finbarrm, 1981; Georgiannou et.al. 1991; Ruggeri, 2008; Clayton *et.al*. 2009; Clayton *et.al*. 2009; Goktepe and Sezer, 2010; Carrera et al. 2011; Ruggeri *et.al*. 2016). The level of participation in the transfer of inter-particle contact stresses by different particle types and sizes within the soil matrix dictates the stress–strain behaviour and the resistance it can offer under different loading conditions (Thevanayagam *et.al.* 2002; Cabalar and Hasan, 2013; Ruggeri *et.al*. 2016).

Although a significant portion of natural soils are poorly graded, consisting of particles of a range of different sizes ranging from clay (≤0.002mm) to boulders (>630mm), geotechnical practice broadly classifies soils as being either fine grained or coarse grained. Morainal deposits (e.g. tills), hillwash deposits (e.g. colluvium) and submarine mass flow deposits (e.g. diamictite) are just some examples of broadly graded composite (i.e. clay-gravel mix) materials. A number of researchers have investigated the influence of granular content on the engineering behaviour of composite soils (e.g. Holtz and Willard, 1956; Muir-Wood and Kumar, 2000; Vallejo and Mawby, 2000; Ni *et.al*. 2004; Jafari and Shafiee, 2004; Prakasha and Chandrasekaran, 2005; Long and Menkiti, 2007; Cabalar and Hasan, 2013; Ruggeri *et.al*. 2016). It is generally assumed that the overall behaviour of these soils is controlled by the predominant material, broadly described as “matrix dominated” where the granular inclusions are in suspension and “grain dominated” where the grains are physically in contact. The percentage of granular inclusions required for a composite soil to behave like a grain dominated material is variable and depends upon the grading (Ruggeri *et.al*. 2016). One of the key aspects of the behaviour of composite soils is the interaction between the clay matrix and the solid inclusions, with respect to the volumetric responses and consequently the strength and deformation characteristics. Muir-Wood and Kumar, 2000 examined the impact of granular inclusions by varying the volumetric percentage of the two components (i.e. clay and sand). They suggested that externally measured volumetric responses were indicative of overall sample response, however *“different things were*

happening in the filler material" (i.e. clay matrix). Influence of granular inclusions in compacted fine soils was also investigated by Jafari and Shafiee (2004), who concluded a heterogeneous void distribution in clay matrix. The purpose of this article is to investigate the aspect of heterogeneous void distribution through a series of consolidated undrained compression tests on reconstituted composite materials with varying percentages of solid inclusions. The effect of grain shape is also investigated, through comparison of responses from kaolin samples included with either uniformly graded angular basalt or smooth stainless steel ball bearings.

EXPERIMENTAL PROGRAMME

In the investigations, the samples were formed from a slurry state containing solid inclusions of two different shapes. Two types of solid inclusion were investigated; (a) uniformly graded crushed basalt (Figure 1a) passing through a 3.1mm sieve and retained on 2.3mm sieve, and (b) 3mm diameter smooth stainless steel balls. The shape of the crushed basalt is described as angular (Barrett, 1980) and the ultimate angle of internal friction of the crushed basalt ϕ'_{ult} was 37°. The measured repose angle of heap of ball bearing (in wet conditions) was 16°. Since the specific gravities of the basalt and the kaolin are generally similar ($G_{s(kaolin)}$ = 2.65 and $G_{s(basalt)}$ = 2.75), it was reasonable to assume that the percentages of solid inclusions, based on the dry masses of each component is the same as the volumetric percentages. The percentages of granular content, in the case of basalt, were: 0%, 20%, 40% and 60%. The samples with and without solid inclusions were initially consolidated to various effective confining pressures ranging from 100kPa to 1300kPa. When using ball bearings, the required mass of ball bearings was calculated by correcting for the density of ball bearings in relation to that of the basalt. For example, in the case of basalt, 400g of kaolin dry powder was mixed with 100g of basalt to represent 20% sold inclusions. As the density of the stainless steel (7.60Mg/m^3) was considerably higher than basalt (2.75Mg/m^3), 276g of steel was added to the kaolin of the same mass so that, for a given volume of kaolin, the same percentage of basalt and steel inclusions were included in each sample. The kaolin slurry (without granular inclusion) was mixed at 1.5×LL (Liquid Limit =

70%) and the required amount of solids was added to the slurry. There was a concern that the ball bearings could sink into the weak clay slurry under their own weight, however the strength of the slurry was sufficient enough to support them and prevented the ball bearings from accumulating at the base of the samples. This was confirmed by spreading ball bearings on the surface of slurry in a clear pot, covered with cling film and observing their positions over a period of three days. Figure 1b shows a confirmation that heavy particles (ball bearings) did not sink to the bottom of the saturated kaolin slurry. The thoroughly mixed slurry was then immediately consolidated one-dimensionally to a vertical pressure of 200 kPa in a sampling chamber of 50mm internal diameter. The slurry was allowed to consolidate for two days, although the subsequent triaxial testing (discussed later) confirmed that a consolidation time of 12 hrs was sufficient for complete dissipation of excess pore water pressure. Figure 1c shows a thin section taken on a sample with 60% basalt content that was isotropically consolidated in the triaxial cell to 1300 kPa which confirms the gravel particles were generally isolated. It is possible that a granular content more than 60% may have resulted with a sample having gravel-gravel contacts. The sample was subsequently extruded and trimmed to a height of 100mm. Several trials were initially carried out (on both basalt and ball bearing at different percentages of inclusion) to optimise the sampling process. These trials provided information concerning the volume of slurry required to prepare samples of approximately 100mm in height.

The void ratio of the matrix e_m was calculated using the following relationship:

$$e_m = \left[\frac{\Delta v + \left(\frac{M_{fw} - M_{fd}}{\rho_w} \right)}{\frac{(1-\alpha) M_{fd}}{\rho_s}} \right]$$

where Δv is the volume change during subsequent compression in triaxial cell. M_{fw}, M_{fd}, α, ρ_w, *and* ρ_s are final wet mass, final dry mass, percentage of clay content, density of water and density of clay

Accepted manuscript doi:
10.1680/jgeen.17.00131

respectively. In the case of ball bearing, necessary corrections were made to determine the dry kaolin in the composite material having particles with a much higher specific gravity. As shown in the equation the void ratio was back calculated from the final void ratio at the end of testing. The variation in the initial specific volume of the samples (after the initial preparation) was ±0.03. It was ensured that the pore water pressure parameter (B) was greater than 0.95 prior to consolidation and shearing. This was achieved by increasing the cell pressure and the back pore water pressure in stages (the difference between them was about 15 kPa) in the triaxial cell. A B-value of 0.95 was achieved at back pore water pressure of 150 kPa, though as a norm the back pore water pressure was maintained at 200 kPa during the consolidation stage. The samples were consolidated to various mean effective stresses under isotropic stress conditions (100kPa, 200kPa, 400kPa, 800kPa and 1300kPa) prior to undrained compression using the strain control method. The undrained compression with pore water pressure measurements was preferred as the suitable testing option for evaluating the impact of granular inclusions in clay-based materials, as any breakdown of structure would lead to the development of excess pore water pressure which can be easily identified rather than volume change response in fully drained compression. The end conditions of the samples are typical of any standard testing procedures whereby the top condition was free to move and the bottom was fixed.

A limited number of additional tests were carried out on the composite materials. In these tests: (a) kaolin (prepared at 55% water content) was mixed with 20%, 40% and 60% uniformly graded basalt inclusions and directly consolidated, in stages, in standard one-dimensional consolidation cells (70 mm diameter and 46 mm high) to 800kPa, and (b) the kaolin slurry prepared at 1.5×LL was mixed with approximately 40% inclusions and consolidated, in stages, in a Rowe cell (254 mm diameter and 300 mm high) to 800kPa. In case of the latter test (i.e. (b)), the granular inclusion was not basalt, but a foam (BS3 type foam, stiffness 25MPa, unit weight 0.13Mg/m^3), broken into angular pieces having sizes between 28mm and 50mm. The intention of this investigation was to assess directly the heterogeneous voids distributions in the composite material.

Accepted manuscript doi:
10.1680/jgeen.17.00131

RESULTS AND DISCUSSION

Compression

The samples, prepared for the main investigations were progressively compressed under isotropic stress conditions (in a standard triaxial cell) from 100kPa to 1300kPa and the relevant observations are shown in Figure 2 in semi-log plots. It is common practice to use the global void ratio as a tool to understand the pressure-void ratio relationships and the shear strength. However, this method may not be sufficient to fully explain the response of composite materials, as different behaviour may occur at a micro level (Muir-Wood and Kumar, 2000; Ni *et.al.* 2004, Thevanayagam *et.al*. 2002; Cabalar *et.al*, 2013; Ruggeri *et.al*. 2016). In this study, the void ratio was calculated based on the volume of voids in the clay matrix (represented by e_m) and the solid volume of clay alone, assuming the water to be entirely contained within the clay matrix.

The pressure-void ratio (e_m) relationship for samples with uniformly graded basalt inclusions was significantly affected by the presence of granular inclusions (Figure 2a). The clay sample with 60% inclusions subjected to approximately 1300kPa, for example, achieved a similar matrix void ratio to the sample without any inclusions, but subjected to 200kPa of mean effective stress (see 0% Gravel plot). The slope of the normal compression line λ (based on natural logarithm) marginally varied from 0.2 to 0.22 when the granular inclusion was varied from 0% to 60%. The first loading point (i.e. under 100 kPa) was not included in the determination of λ as the early stages of the compression curves were affected by the stress history that the samples have had during the initial formation in the one-dimensional consolidation chamber. The specific volume of the clay matrix (at 60% granular content), at a consolidation pressure of 1300kPa was about 2.26. However, the maximum void ratio of the basalt (under loose state at 100% granular content) would be around was 1.20, which confirms that the granular inclusions were not in contact and this was also confirmed by an examination of the thin section (Figure 1c). The thin sections of this material (after isotropic consolidation to 1300 kPa) have,

Accepted manuscript doi:
10.1680/jgeen.17.00131

however, shown some isolated contacts between the particles. The volumetric responses of the composite material containing steel ball bearings were distinctively different. The positions and the slopes of the normal compression lines were not significantly affected by the presence of up to 40% ball bearings (Figure 2b). A possible reason for this is explained later in this article. A significant change in the position of the normal compression line was, however, observed with 60% inclusions.

There was a concern that the observed phenomena were only prevailing under isotropic loading and or that they occurred from the start of one-dimensional consolidation during the sampling process. In order to assess this, three one-dimensional consolidation tests were carried out on samples having 20%, 40% and 60% granular content. In these tests, samples were loaded from 50 kPa to 800 kPa in one-dimensional consolidation cells. The observed performances are shown in Figure 3 where the solid data points refer to the observations from one-dimensional consolidation tests and the open data points refer to the information presented in Figure 2a. It should be noted that the data presented for the one-dimensional loading tests in Figure 3 are based on vertical stresses (σ'_v) and not based on mean effective stress p' whereas the comparable data extracted from Figure 2a are based on the isotropic stresses. The information gathered from the one-dimensional consolidation tests also intuitively confirms that the addition of granular inclusions leads to increased void ratio of the clay matrix when compared to clay without granular inclusions, at a given pressure. There appears to be some differences between the positions of the normal compression lines between the two different types of loading, however this can be attributed to the nature of the loadings (i.e. isotropic in triaxial cell and anisotropic in one-dimensional consolidation cell). Additionally, a small amount of side friction would be expected in the one-dimensional consolidation tests, between the sample and the rigid container. This effect is not taken into consideration in the present investigations. The observed differences in the matrix void ratios in the presence of granular inclusions are attributed to: (a) physico-chemical forces and (b) fabric and structural changes. These two aspects are further discussed below.

Accepted manuscript doi:
10.1680/jgeen.17.00131

Physico-chemical forces: Clay particles carry net negative charges at their surfaces due to the isomorphous substitution in the crystal lattice (van Olphen 1977). The specific surface area of kaolinite is in the order of 10-20 m^2/g and the cation exchange capacity is about 3 meq/100g (Lambe and Whitman 1969). The magnitude of the electrical charge is directly related to the specific surface area. In the kaolinite mineral there is a very small amount of isomorphous substitution (Lambe and Whitman 1969). The interaction between the negatively charged surfaces of the clay particles, metal ions and water is responsible for the formation of electrical double layer surrounding the clay particles. The magnitudes of attractive forces arising from the van der Waals and Coulombic attraction and the repulsive force stemming from the electrical double layer interaction between clay particles depend upon the specific surface area, the pore fluid characteristics and the properties of the fluid (dielectric constant, concentration and pH) in contact with the clay (Sridharan and Jayadeva, 1982; Mitchell and Soga 2005). In case of the mineral kaolinite, the thickness of the diffuse double layer is relatively thin as compared to that of other minerals, such as montomorillonite and illite (Lambe and Whitman 1969). In the absence of an appreciable repulsive force, the factors determining the volume change behaviour of kaolinite are the frictional resistance, the fabric and magnitude of the attractive force (Sridharan and Rao 1973). An increase in the cation valence and decrease in the dielectric constant and pH of the pore fluid tend to increase the interparticle attractive forces and favour higher flocculation in case of kaolinite. However, these effects did not appear to have any significant influence on the physico-chemical forces in the clay composite systems considered in this study. Therefore, the factors determining the volume change behaviour of kaolin/basalt and kaolin/ball bearing are primarily attributed to the frictional resistance and the fabric of the clay which is further explored below.

Accepted manuscript doi:
10.1680/jgeen.17.00131

Fabric and structural changes: The clay matrix and the isolated granular inclusions are illustrated in Figure 4. In the absence of inclusions, the clay matrix does not experience significant shear strain under isotropic stress conditions, assuming that the clay matrix possesses isotropic stiffness properties. Although isotropic stress conditions are maintained on the boundary of the samples, the presence of angular inclusions creates an intense shear zone in the clay surrounding the inclusion due to the variation in stiffness between the individual materials and the mobility of the granular inclusions. Since the clay matrix is normally consolidated, the clay surrounding the solid inclusions undergoes strain hardening, resulting in a reduction in void ratio. If the inclusions are close enough, this hardening process forms strong bridges between the inclusions (Figure 4b). This phenomenon was also postulated by Jafari and Shafiee (2004); however, in their studies the samples were compacted prior to further investigations. The formation of bridges is also affected by concentration of stresses in the clay between the solid inclusions. The development of such bridging is progressive with increasing consolidation pressure. As this arching/bridging mechanism develops, the clay matrix enclosed by the solid inclusions does not experience the full extent of the externally applied pressure and it becomes consolidated under a lower pressure. The void ratio of the material in this region could therefore be significantly higher than in the bridge. Such bridge formation is significantly influenced by the particle shape and can be considered to be very intensive in angular particles. If the particles are smooth and rounded (such as ball bearings), the intensity of the shear strain surrounding the particles and concentration of the stresses between the particles are significantly reduced and therefore the impact of such granular inclusions in the matrix void ratio can be limited as observed in Figure 2b. It should be also pointed out that the inclusion of granular contents will reduce the overall void ratio (e) and the compressibility of the composite material, but the contrasting observation is that the compressibility of the clay matrix (λ) generally remained unchanged. This would have a significant impact on excess pore water pressure development if such materials are loaded under undrained conditions. This is further discussed later in the article.

Direct evidence of heterogeneous pore void distribution was obtained by measuring the distribution of void ratio in the sample. Due to the difficulties in assessing the water content distribution in 50mm diameter samples with basalt inclusions of smaller particles, two separate tests were carried out in a Rowe Cell (sample diameter = 254mm). The samples without and with granular inclusions (40% foam by volume of solids) were consolidated to 800kPa of vertical stress and the pressure-volume relationships for these two tests are illustrated in Figure 3. It is again remarkable that the position of the NCL for the sample included with 40% foam falls above the NCL for 0% granular inclusions. The position of this line remained close to the normal compression lines obtained for isotropically or one-dimensionally compressed samples having 40% granular inclusions. At the end of the tests, both samples (with and without granular inclusions) were extruded from the Rowe Cell and cut by band-saw at mid height to assess the void ratio distributions. The relevant observations are shown in Figure 5a (re-drawn illustration based on a digital image of the cut-surface). Figure 5a illustrates the locations of the granular inclusions (Foam) within the clay matrix following the test. Figure 5b shows the distributions of void ratio at various locations. Once again the observations have confirmed a strong heterogeneous void distribution in the sample with granular inclusions was also postulated by Jafari and Shafiee (2004).

In order to further confirm the above observations, several SEM images were acquired (5000x magnification) on the sample having 60% basalt inclusions, isotropically consolidated in the triaxial cell to a pressure of 1300kPa (Figure 6). Based on visual observations marked by boundaries, the packing of clay particles was tight and close together at location 2 (i.e. between the granular inclusions), whereas at locations 1 and 3 (i.e. away from the inclusions), the clay particles were relatively loose, supporting the hypothesis. However, it is agreeable that the evidences shown in Figure 6 are only qualitative and a quantification of the varying pore size distribution would require further investigation in the form of 3D SEM images. In addition, discrete element modelling (DEM) could numerically validate the hypothesis presented above.

Accepted manuscript doi:
10.1680/jgeen.17.00131

Stress-strain behaviour

The presence of granular inclusions generates heterogeneous pore void distributions and therefore the meaning of "undrained compression" is questionable as there can be re-distribution of pore water in the voids, even though the overall volume of the sample is maintained constant. This can make the stress-strain behavior complex, and identifying the critical state can be difficult. Muir-Wood and Kumar (2000) carried out an extensive investigation on kaolin-sand mix at various proportions and the samples were sheared under drained and undrained conditions. They used the maximum q/p' ratio as an indication of critical state, although there was no evidence presented in the article to confirm if an actual critical state was obtained. Carrera *et.al*. (2011) carried out investigation on Stava tailing in which the samples were reconstituted with different percentage of sand and fine particles in order to examine the liquefaction potential of composite materials. These authors also assumed that conditions at the maximum q/p' ratio can be an indication of the critical state. In a recent study, Ruggeri *et.al*. (2016) carried out a large number of tests on composite materials prepared at different percentages of granular inclusion and used the same technique to identify the critical state. In this study, it was therefore assumed that the critical state was reached at maximum stress ratio (σ'_1/σ'_3), which also corresponds to the maximum q/p'.

Figure 7 (a,b,c) illustrates the stress-strain behaviour of clay containing various percentages of uniformly graded basalt, subjected to 1300kPa of initial consolidation pressure. The strain is based on the axial displacement in relation to original height of the sample. The behaviour observed in the test without inclusions is typical of normally consolidated clay, with the sample reaching critical state at about 14% axial strain. However, the behaviour changed as the percentage of granular content was increased. The samples without inclusions failed in shear plane (physically observed and indicated on Figure 7a) and the deviator stress gradually approached the residual state. The sample with 20% granular content also failed on shear plane; however, the samples with 40% and 60% granular content continued to bulge, while the deviator stress gradually reduced post-peak. This indicates that the

alignment of particles under large strain is affected by the presence of inclusions. The development of pore water pressure during undrained compression is also affected. The pore water pressure was found to increase post-peak in the sample with 40 and 60% inclusions.

Thin sections obtained on samples with 60% inclusions (isotropically compressed to 1300kPa), demonstrated that the inclusions were generally isolated with only marginal interactions. It is therefore likely that inter-particle friction does not significantly contribute to the overall strength. The sample with 60% granular content consolidated to 1300kPa reached a maximum deviator stress of 620kPa, which is only 40kPa less than the sample without inclusions (Figure 7a). In the samples with 20% and 40% inclusions, the peak stresses were 590kPa and 550kPa respectively. There are two aspects that require further explanation: (a) overall, the peak deviator stresses of the samples containing granular inclusions are high if it is assumed that the strength is only provided by the clay matrix and (b) if the poorly compressed clay were to be responsible for the reduced strength, then the peak stress of the sample with 60% inclusions should be lower than that of the samples containing fewer inclusions. The arching effect, as discussed above, could have contributed to the high strength observed in samples with inclusions. It is possible that continued shearing of the samples beyond their peak strengths destroyed these arches and exposed the enclosed clay to the externally applied pressures. If this were to be the case, the pore water pressure should continue to increase as shearing progressed, which was actually observed in the samples with inclusions (Figure 7b). The relatively high deviator stress measured in the sample with 60% granular content can be explained by isolated shearing between the aggregates. Figure 7c shows the stress ratio (σ'_1/σ'_3) during the shearing process at initial consolidation pressure of 1300 kPa.

Figure 7d shows the stress paths for the CIU tests carried out on the samples with and without the inclusions. In samples with granular contents of 20% and 40%, the peak state (also assumed to be the critical state, based on the maximum stress ratio and indicated by closed data points) correlates

reasonably well with the critical state line, identified from tests without inclusions, indicating that shearing was taking place in the clay matrix. However, in the case of 60% gravel, the critical state line (indicated by open circular data points) lies above the same identified from 0, 20% and 40% granular inclusion, implying the possibility of isolated shearing between the granular inclusions. In the case of 0% granular inclusion, the slope of the post-peak stress path (i.e. approaching the residual state) is approximately 3. Similar observations have been reported by Georgiannou and Hight (1994). However, as the percentage of granular inclusions increases, the slope of the stress path reduces. For example, the post-peak stress path of the composite material with 20% granular content is approximately 2.9 and that for 40% and 60% granular contents are 2.05 and 1.85 respectively. These observations also agree with Carrera *et.al.* (2011). A reduction in the post-peak slope is largely attributed to continued development of pore water pressure as the shearing progressed through post peak state.

Figure 8 shows the void ratio (e_m) plotted against the mean effective stress at critical state. For clarity, the data are presented in two separate figures: Figure 8a shows the NCL and CSL for 0% and 40% granular inclusions and Figure 8b shows the same for 20% and 60% granular inclusions. It is remarkable that the NCL are parallel to CSL at all percentages of granular inclusions and that, in general, the spacing between them remained unchanged. Muir-Wood and Kumar (2000), presented data obtained on composite material subjected to fully drained shearing. In their studies the volumetric strains were generally unaffected by the percentage of granular inclusions. Although they did not present the NCL and CSL directly, their data also implies that the NCL may be parallel to the CSL at a given percentage of granular inclusions. Ruggeri *et.al*. (2016) presented e_m (referred to as specific volume, v_c) for various combinations of fine-granular mix. Since all their tests were carried out at 400kPa of consolidation pressure, it was not possible to locate the NCL or CSL for a given granular inclusions. However, it is clear that the e_m at critical state increases with the size of the granular inclusions, which agrees favourably with the observations presented here.

Accepted manuscript doi:
10.1680/jgeen.17.00131

Unlike the tests with basalt inclusions, the peak deviator stresses of samples with 20%, 40% and 60% ball bearings are similar (Figure 9). This agrees with the earlier observations where the presence of up to 40% ball bearings did not have any significant influence on the position of the normal compression lines. The pore water pressure responses are generally similar among tests containing 0, 20 and 40% inclusions (contrast to the observations made in basalt inclusion, Figure 7b) and significantly different at 60% ball bearings (Figure 9b). Unlike the test on 60% basalt (Figure 7a), the effect of localised shearing was substantially reduced on tests with the equivalent ball bearing content. Samples with 20% and 40% ball bearings failed in shear as the samples continued to deform, whereas the sample with 60% ball bearings continued to bulge. As discussed in the case of granular inclusions, the slope of the post peak stress path is 3 for 0% granular inclusions and remained approximately same for 20% and 40% ball bearing content. This slope reduced to 2.0 as the percentage of ball bearing was increased to 60%.

Figure 10 shows the variation of the effective angle of internal friction at the critical state (based on the maximum stress ratio), $\phi'_{cv.}$ The ϕ'_{cv} for kaolin is approximately 21°. The inclusion of 20% and 40% basalt marginally reduced ϕ'_{cv} by 0.7°; however, at 60% inclusions ϕ'_{cv} increased by 2.3°. The inclusion of 20% ball bearings in place of basalt reduced the ϕ'_{cv} by 3.2° (to 18°); however, further increase in the inclusion content increased ϕ'_{cv} to 19.9° at a ball bearing content of 60%. Ruggeri *et.al.* (2016) reported a progressive increase in the angle of internal friction as the granular content was reduced from 100% to 0%. However, only a small increase of ϕ'_{cv} was observed up to about 30% granular inclusions. The present investigation confirms this observation as ϕ'_{cv} generally remains constant up to about 40% granular content. The increase in the friction angle at 60% granular content can be attributed to isolated granular contacts (also observed in thin section). The frictional resistance between basalt and kaolin can be taken as the minimum friction angle of the two individual components of the composite material. In the present investigation it is kaolin which controls the minimum friction angle. However, when the ball beings were included as the solid inclusion, the

interface friction angle between ball bearings and the surrounding clay is much lower than the ϕ'_{cv} of kaolin. This may explain why the friction angle initially dropped as the percentage of ball bearing was increased.

CONCLUSIONS

Investigations were carried out on samples of kaolin with granular inclusions of crushed angular basalt and smooth ball bearings to examine their effect on the compression and strength characteristics of clays. Isotropic compression and one-dimensional consolidation tests revealed that granular inclusions have an influence on the pressure-void ratio characteristics of the clay matrix. It is hypothesized that the zone surrounding the solid inclusions experiences intense shear deformation, leading to the formation of arches between inclusions. As this arching/bridging mechanism develops, the clay matrix enclosed by the solid inclusions does not experience the full extent of the externally applied pressure and it becomes under-consolidated and consequently heterogeneous void distribution in the clay matrix which was independently validated using SEM and water void ratio measurements. This phenomenon was found to be subdued when the surface of the granular inclusion was smooth, which suggests that particle shape has a considerable influence on the volumetric behaviour of composite materials.

Increasing the granular content resulted in an increase in peak strength during shear loading on samples with basalt inclusions. This observation could also have been a product of the bridging mechanism between granular inclusions. Continued shearing of samples leads to destruction of these bridges, possibly exposing the enclosed clay to the externally applied pressures. This has resulted in a continued build-up of the pore water pressure even though the samples appeared to have reached the critical state. In kaolin–basalt mix, there appears to be no significant change in friction angle until the granular content was 60%. Particle

shape was also found to have a considerable influence on the behaviour of the samples during shearing. The critical state friction angle reduced noticeably when the ball bearing contents were increased up to 40%.

ACKNOWLEDGEMENT

The authors also wish to thank Mr Deacy, P J Carey Ltd, UK for continuing their support for the geotechnical engineering research at Queens' University Belfast.

Accepted manuscript doi:
10.1680/jgeen.17.00131

REFERENCES

Barrett PJ (1980) The shape of rock particles, a critical review. Sedimentology **27**: 291-303.

Cabala AF and Hasan RA (2013) Compressional behaviour of various size/shape sand–clay mixtures with different pore fluids. Engineering Geology **164**: 36-49.

Carrera A, Coop M and Lancellotta R (2011) Influence of grading on the mechanical behaviour of Stava tailings. Géotechnique **61(11)**: 935–946.

Clayton CRI, Abbireddy COR and Schiebel R (2009) A method of estimating the form of coarse particulates. Geotechnique **6**: 496-501.

Clemence SP and Finbarr AO (1981) Design Considerations for Collapsible Soils. Journal of the Geotechnical Engineering Division, ASCE **107(GT3)**: 305-317.

Goktepe AB and Sezer A (2010) Effect of particle shape on density and permeability of sand. Geotechnical Engineering **163**: 207-320.

Georgiannou VN, Hight DW and Burland JB (1991) Behaviour of clayey sands under cyclic triaxial loading. Geotechnique **41(3)**: 383-393.

Holtz WG, and Willard M (1956) Triaxial shear characteristics of clayey gravel soils. Journal of Geotechnical Engineering, ASCE **82**: 143-149.

Jafari MK and Shafiee A (2004) Mechanical behaviour of compacted composite clays. Canadian Geotechnical Journal **41**: 1152-1167.

Lambe WT and Whitman RV (1969). Soil mechanics. Wiley, New York

Long M and Menkiti CO (2007) Geotechnical properties of Dublin Boulder Clay. Géotechnique **57(7)**: 595–611.

Mesri G and Olson RE (1970). Mechanism controlling the permeability of clays. Clays and clay minerals **19**: 151-158.

Mitchell JK and Soga K (2005) Fundamentals of soil behaviour, 3rd edn. Wiley, New York.

Muir-Wood D and Kumar GV (2000) Experimental observations of behaviour of heterogeneous soil. Mechanics of frictional materials **5**: 373-398.

Ni Q, Tan TS, Dasari GR and Hight DW (2004) Contribution of fines to the compressive strength of mixed soils. Géotechnique **54(9)**: 561–569.

Prakasha KS and Chandrasekaran VS (2005) Behavior of marine sand-clay mixtures under static and cyclic triaxial shear. J. Geotech and Geoenvironmental Eng, ASCE **131(2)**: 131–122.

Ruggeri P (2008) Comportamento meccanico di un terrenocomplesso a granulometria eterogenea. PhD thesis, Università Politecnica delleMarche, Ancona, Italy (in Italian).

Ruggeri P, Segato D, Fruzzetti VME, and Scarpelli G (2016) Evaluating the shear strength of a natural heterogeneous soil using reconstituted mixes. Geotechnique **66**: 941-946.

Soroush A and Jigheh HS (2009) Pre- and post-cyclic behavior of mixed clayey soils. Canadian Geotechnical Journal **46**: 115-128.

Sridharan A and Jayadeva MS (1982) Double layer theory and compressibility of clays. Geotechnique **32**: 133–144.

Sridharan A and Rao GV (1973) Mechanisms controlling volume change of saturated clays and the role of effective stress concept. Geotechnique **23(3)**: 359-382.

Thevanayagam S, Shenthan T, Mohan S and Liang J (2002). Undrained fragility of clean sands, silty sands and sandy silts. J. Geotech and Geoenvironmental Eng, ASCE **128(10)**: 849–859.

Vallejo LE and Mawby R (2000). Porosity influence on the shear strength of granular material– clay mixtures. Engineering Geology **58**: 125-136.

van Olphen H (1977) An introduction to clay colloid chemistry: for clay technologists, geologists and soil scientists, 2nd edn. Interscience, New York.

Accepted manuscript doi:
10.1680/jgeen.17.00131

Figure 1 Basic information on the sample preparation and granular contents
Figure 2 Pressure-matrix void ratio relationships under isotropic stress conditions
Figure 3 Pressure-matrix void ratio relationships under isotropic and onedimensional loading conditions
Figure 4 Shear zone around the particles
Figure 5 Void ratio distributions (Rowe cell consolidation with foam 0% and 40%)
Figure 6 SEM images of clay matrix
Figure 7 Stress-strain behaviour and stress paths: Uniformly graded basalt
Figure 8 Pressure-volume relationship at critical state: Uniformly graded basalt
Figure 9 Stress-strain behaviour and stress paths: Ball bearings
Figure 10 Effective angle of internal friction and granular contents

Accepted manuscript doi:
10.1680/jgeen.17.00131

(a) Uniformely graded basalt

(b) Slurry supporting ball bearings

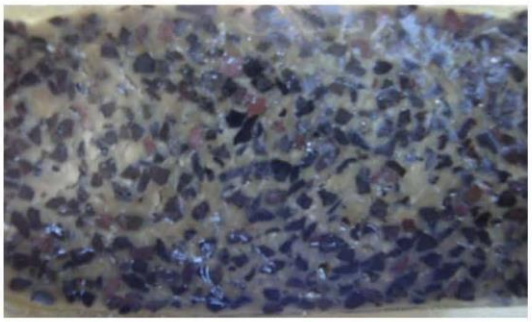

(c) 60% gravel, sample compressed to 1300 kPa (a thin section)

Figure 1

Fig 1.jpg

Accepted manuscript doi:
10.1680/jgeen.17.00131

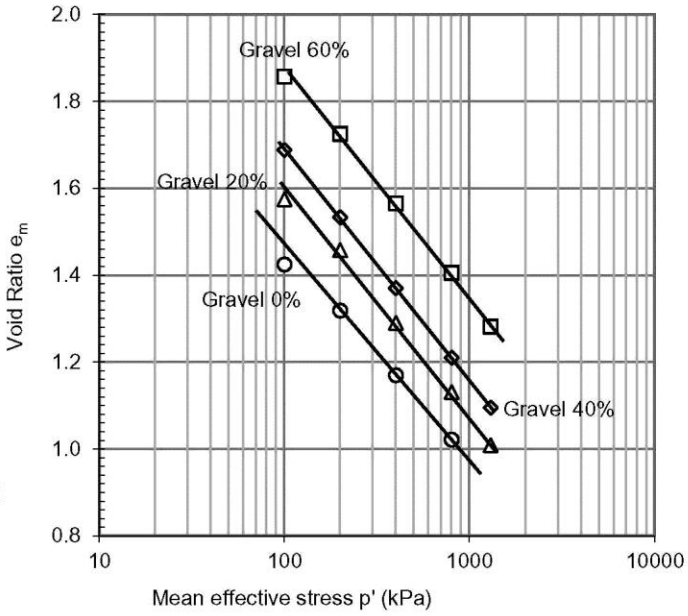

(a) Unformly graded

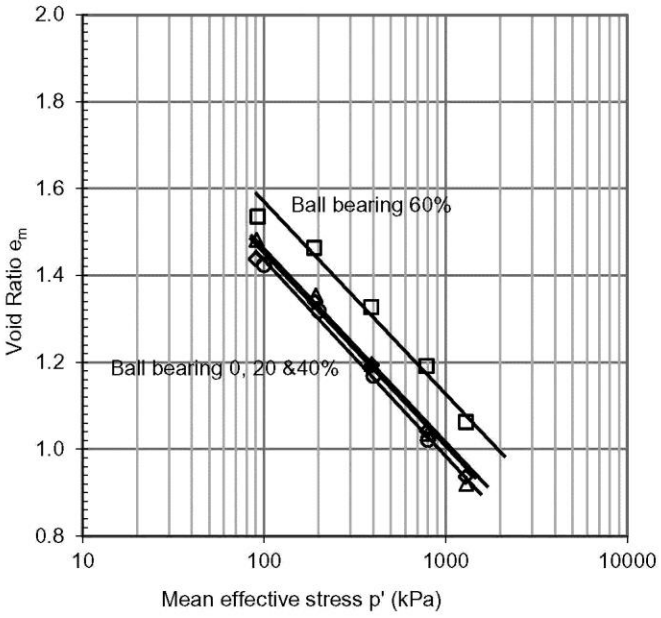

(b) Ball bearings

Figure 2

Fig 2.jpg

Accepted manuscript doi:
10.1680/jgeen.17.00131

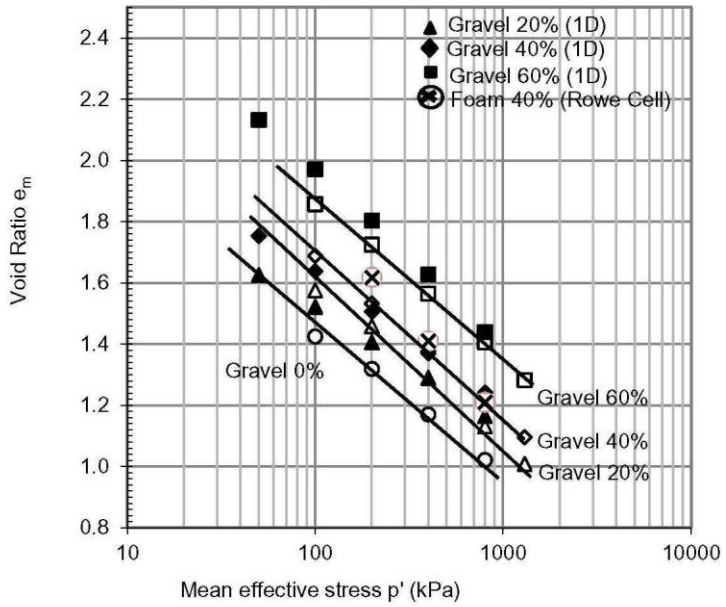

Figure 3

Fig 3.jpg

Accepted manuscript doi:
10.1680/jgeen.17.00131

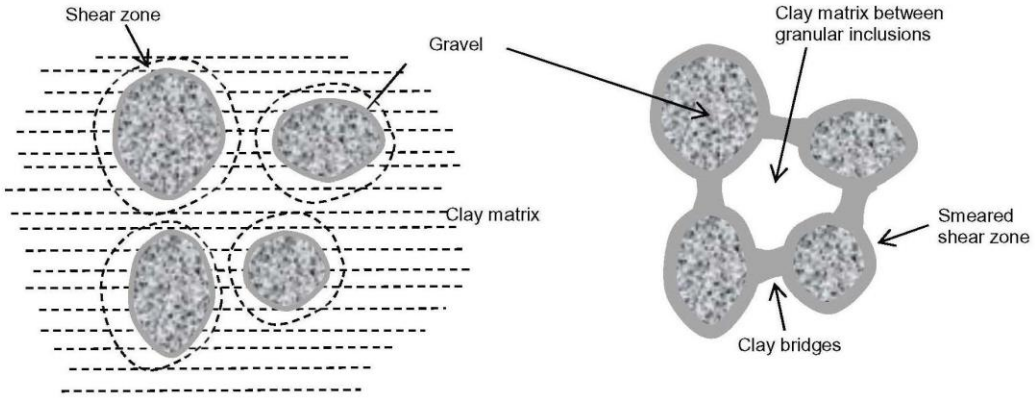

(a) Shear zone

(b) Bridging between solid inclusions

Figure 4

Fig 4.jpg

Accepted manuscript doi:
10.1680/jgeen.17.00131

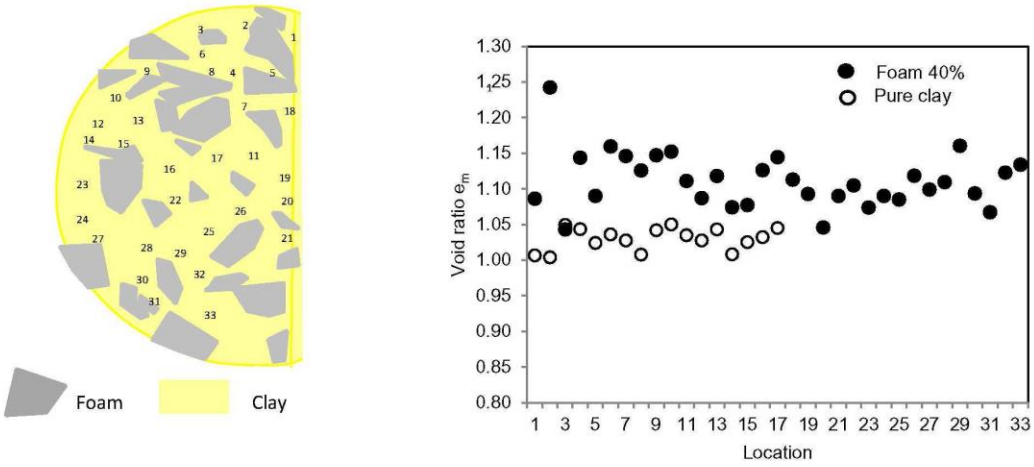

(a) Cut section of the sample in Rowe cell Containing 40% Foam

(b) Void ratio distribution

Figure 5

Fig 5.jpg

Accepted manuscript doi:
10.1680/jgeen.17.00131

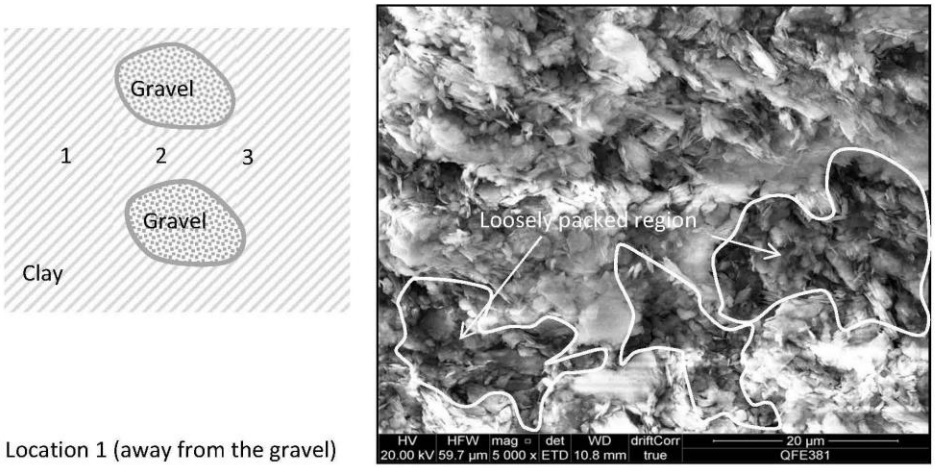

(a) Location 1 (away from the gravel)

(b) Location 2 (between the gravel)

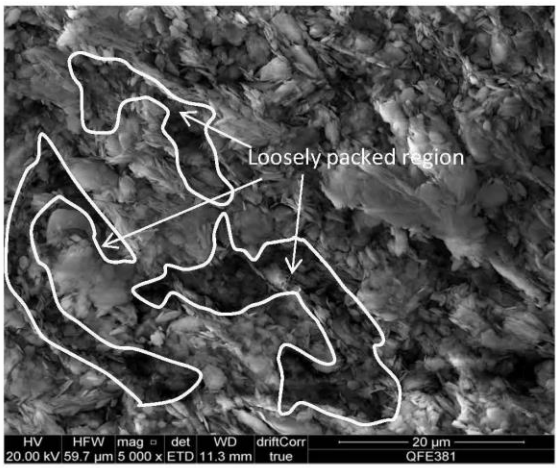

(c) Location 3 (away from the gravel)

Figure 6

Fig 6.jpg

Accepted manuscript doi:
10.1680/jgeen.17.00131

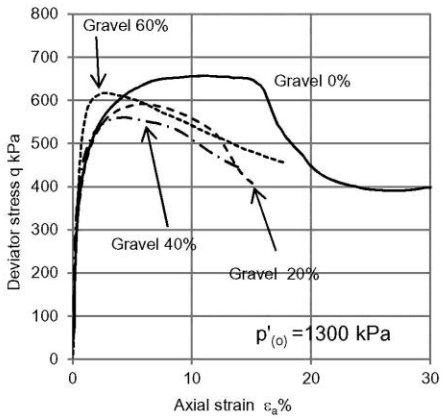

(a) Deviator stress vs axial strain

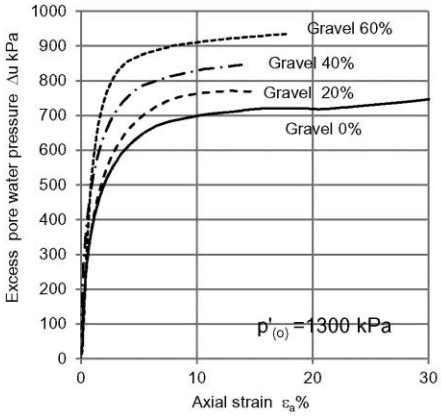

(b) Excess pore water pressure vs axial strain

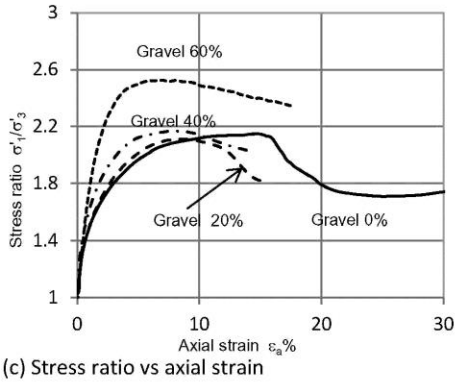

(c) Stress ratio vs axial strain

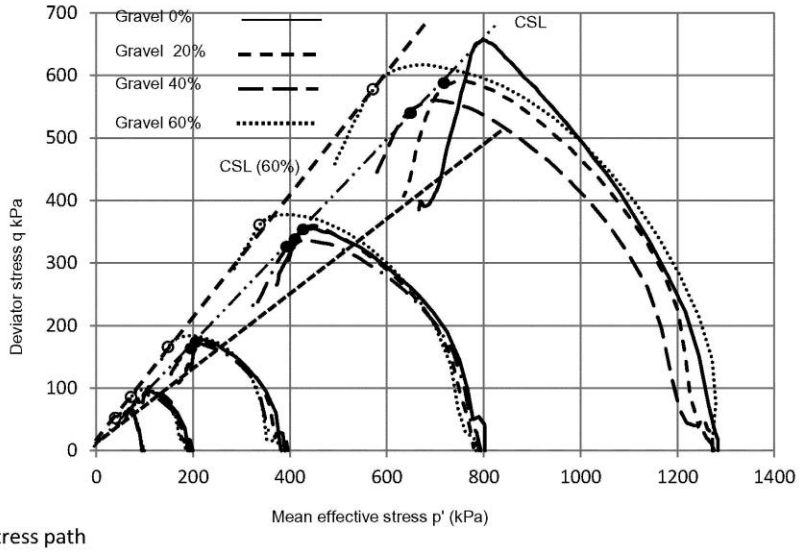

(d) Stress path

Figure 7

Fig 7.jpg

Accepted manuscript doi:
10.1680/jgeen.17.00131

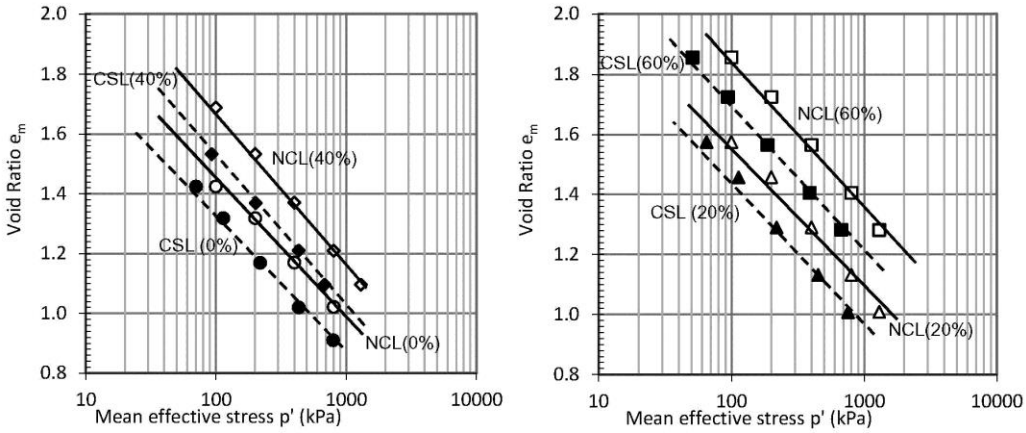

(a) Normal and critical state lines (0 and 40% gravel) (b) Normal and critical state lines (20% and 60% gravel)

Figure 8

Fig 8.jpg

Accepted manuscript doi:
10.1680/jgeen.17.00131

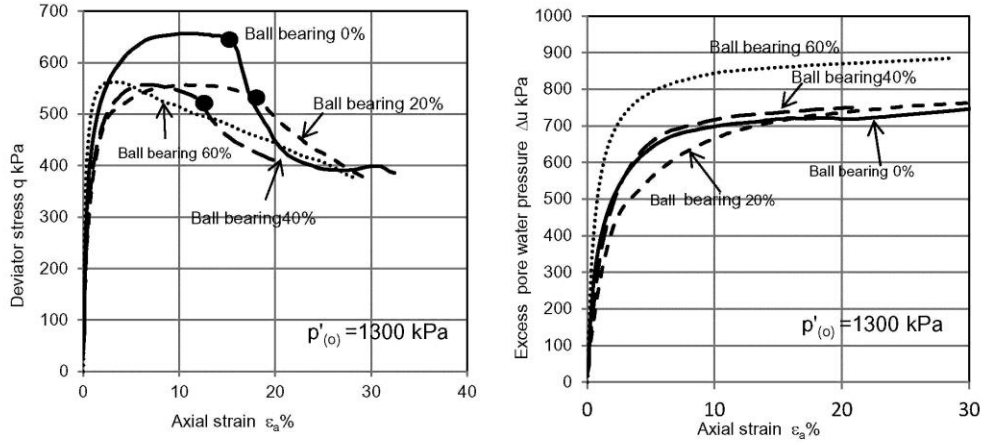

(a) Deviator stress vs axial strain (b) Excess pore water pressure vs axial strain

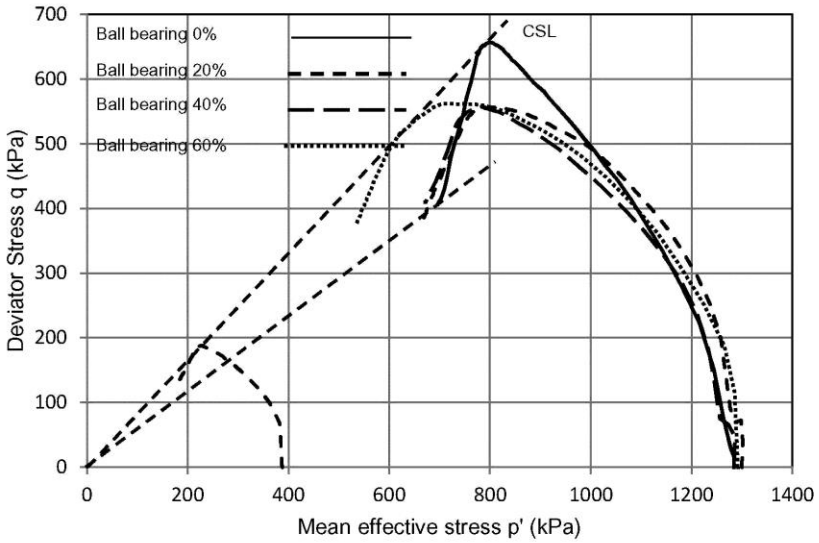

(c) Stress path

Figure 9

Fig 9.jpg

Accepted manuscript doi:
10.1680/jgeen.17.00131

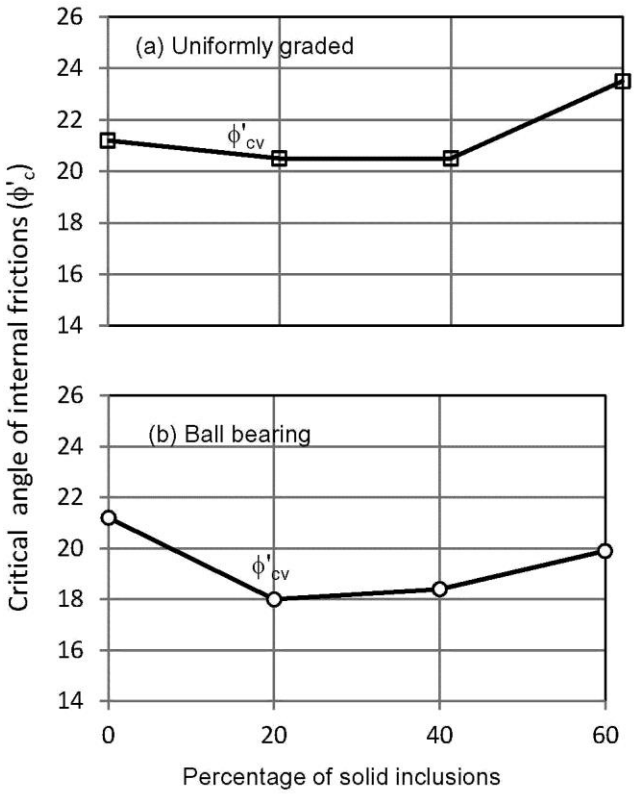

Figure 10

Fig 10.jpg